Chemical Engineering Journal 232 (2013) 346–355

Contents lists available at ScienceDirect

Chemical Engineering Journal

journal homepage: www.elsevier.com/locate/cej

Direct production of highly conductive graphene with a low oxygen content by a microwave-assisted solvothermal method

Tran Van Khai [a,e], Dong Sub Kwak [a], Yong Jung Kwon [a], Hong Yeon Cho [a], Tran Ngoc Huan [b], Hoeil Chung [b], Heon Ham [c], Chongmu Lee [d], Nguyen Van Dan [e], Ngo Trinh Tung [f], Hyoun Woo Kim [a,*]

[a] Division of Materials Science and Engineering, Hanyang University, 17 Haengdang-dong, Seongdong-Gu, Seoul 133-791, Republic of Korea
[b] Department of Chemistry, Hanyang University, 17 Haengdang-dong, Seongdong-Gu, Seoul 133-791, Republic of Korea
[c] H&H Co. Ltd., Chungju National University, 50 Daehak-ro, Chungju-si, Chungbuk 330-702, Republic of Korea
[d] School of Materials Science and Engineering, Inha University, Incheon 402-751, Republic of Korea
[e] Faculty of Materials Technology, Ho Chi Minh City University of Technology, 268 Ly Thuong Kiet Street, Ward 14, District 10, HoChiMinh City, Viet Nam
[f] Institute of Chemistry, Vietnam Academy of Science and Technology (VAST), 18 Hoang Quoc Viet, Caugiay, Hanoi, Viet Nam

HIGHLIGHTS

- Few-layer graphene with a low oxygen content was synthesized by a two-step process.
- Expanded graphite was subjected to solvothermal treatment, followed by microwave radiation.
- The as-fabricated graphene sheets exhibited a high electrical conductivity.

ARTICLE INFO

Article history:
Received 29 March 2013
Received in revised form 25 July 2013
Accepted 31 July 2013
Available online 8 August 2013

Keywords:
Graphene
Solvothermal
Microwave

ABSTRACT

Few-layer graphene (FLG) with a low oxygen content has been synthesized by a two-step process using expanded graphite (EG) as a starting material. EG was subjected to solvothermal treatment, followed by microwave radiation. The FLG had an average thickness in the range of 1.8–2 nm with a lateral size of 3–10 μm. Both Raman spectroscopy and high resolution TEM measurements showed that the sizes of sp^2 carbon domains in graphene oxide (GO) and FLG were estimated to be about 2–5 nm and 10–16 nm, respectively. X-ray photoelectron spectroscopy and Fourier transform infrared spectroscopy spectra revealed that the FLG consisted of several peaks similar to those of EG, which were not observed in GO, indicating the effectiveness of the solvothermal reduction method in lowering the oxygen level. The electrical conductivity of the as-synthesized FLG ismeasured to be 165 S/m, which is much higher than that of the GO (1.2×10^{-4} S/m), possibly due to the larger sp^2 carbon domain size, lower oxygen content, and fewer structural defects. In contrast to the Hummer method, the method is simple, inexpensive, and does not generate toxic gas. This simple method could provide the synthesis of high quality FLG on a large scale.

1. Introduction

Graphene is a single layer of sp^2-hybridized carbon atoms arranged in a two-dimensional hexagonal lattice. Due to their outstanding physical and chemical properties, graphene and its derivatives have attracted tremendous attention for both fundamental science and possible technological applications [1–6]. Graphene-based sheets have been shown to be very promising for high-performance nanoelectronics, transparent conductors, polymer composites, and microscopy support, etc. Currently, various methods have been developed for production of graphene, including chemical vapor deposition (CVD) [7], micromechanical exfoliation of graphite [8], epitaxial growth on electrically insulating surfaces such as SiC [9],physical method [10] and chemical processing [11,12]. Among them, the chemical approach is the most suitable method for economically producing graphene sheets on a large scale.

Currently, the Hummers' method is the most widely used technique for preparing GO [13], which involves oxidation of graphite in the presence of strong acids and oxidants. When oxidized, GO still possess a layered structure, being composed of unoxidized aromatic regions and aliphatic regions, which contain many oxygen functional groups [14,15]. The π-conjugated system in graphene is disrupted by these oxygen-containing functional groups, producing separated nanocrystalline graphene. Since the as-pre-

* Corresponding author. Tel.: +82 10 8428 0883.
E-mail address: hyounwoo@hanyang.ac.kr (H.W. Kim).

1385-8947/$ - see front matter © 2013 Elsevier B.V. All rights reserved.
http://dx.doi.org/10.1016/j.cej.2013.07.123

pared GO is an electrical insulator, various reduction methods have been developed to efficiently recover its electrical property. However, reduced graphene oxide (RGO) still exhibits much lower conductivity than pristine graphene, mainly due to the presence of irreversible defects, disorder and residual functional groups. Moreover, the reduction of GO involves strong reductive agents, such as hydrazine or dimethyl hydrazine, which are highly toxic and dangerously unstable. Therefore, direct thermal annealing at elevated temperatures, or CVD, is required to repair the defects and further remove the residual functional groups in RGO to improve its electrical properties, while eliminating the use of potentially hazardous reducing agents. However, these treatments increase the cost and complexity of the CVD process and they are unfavorable for low-temperature applications.

In order to avoid applying Hummers' method, Liang et al. [16] suggested a vacuum filtration method where reduction-fee thermally conductive surface functionalized multilayer graphene sheets are aligned in water to create paper-like graphene with low defect level and high conductivity. Recently, solvothermal techniques have been employed to produce graphene [17]. Due to their unique features, such as very high self-generated pressure inside the sealed reaction vessel and containment of volatile products, solvothermal techniques are well suited for the preparation of metastable phases. Nethravathi and Rajamathi [18] and Dubin et al. [19] also reported the solvothermal reduction of exfoliated GO in organic solvents. On the other hand, Liang et al. [20] suggested that microwave could reduce defects on graphene sheet and concentration of function groups. However, this method presents the same disadvantages as all synthetic approaches where GO is used as starting material: the sp^3 defects cannot efficiently convert to sp^2 and the remaining oxygen groups [18,21]. Therefore, it is necessary to develop an effective method to directly produce graphene sheets, which have less defects and low oxygen content, resulting in much better conductivity. In this regard, we propose a simple method to produce graphene sheets by means of the microwave irradiated expansion of graphite intercalation compounds, which have been prepared through a solvothermal process. One of the advantages of this synthetic method is its simplicity without toxic chemical agents and harsh oxidation of graphite. Microwaveirradiation facilitates mass production in a short time with little energy cost. Herein, we will show a detailed study of the structure and properties of the obtained FLG, in comparison to those of GO prepared by a modified Hummers' method.

2. Experimental

We used commercial EG as the starting material. This is transformed to a sheet with 2–5 atomic layers, though microwave irradiated expansion following a solvothermal process. This method is simple, inexpensive, produces usable results, and especially, does not generate toxic gas. Briefly, a potassium organic solution was first prepared by adding a stoichiometric amount of potassium hydroxide, 5 g to 50 mL of tetrahydrofuran (THF) organic solvent (i.e., the mass ratio of KOH to THF ≈0.1), and stirred for 24 h at room temperature. Then, 0.5 g EG was added to this solution, and the resulting mixture was transferred to a Teflon-lined autoclave (25 mL) and maintained at 250 °C for 72 h, during which time the mixture was stirred with a Teflon magnetic stirrer. At the same time, the dissolved potassium ion in the solvent is intercalated into the interlayer space of the graphite, forming a black suspension. Next, the reaction products were irradiated by rapid microwave heating for 60–120 s using a commercial microwave oven (Panasonic, model: NE-1054F 1000-Watt – 2450 MHz, 0.8 cubic feet cavity, power source: 120 V, 60 Hz). Then, we can obtain the exfoliated graphene sheets from the irradiated intermediate of alkali metal intercalated EG. The obtained exfoliated graphene nanosheets were then redispersered in HCl (3%) solution with mild sonication for 3 h, and repeatedly washed with distilled water until the pH = 7. To obtain uniform graphene sheets, a low-speed centrifugation at 2000 rpm (5 min) was first used to remove thick sheets. Then the supernatant was further centrifuged at 6000 rpm for 30 min to remove small graphene pieces and water-soluble byproduct. The final sediment was dried and stored in a vacuum oven at 60 °C until use.

For comparison, we prepared GO from EG by a modified Hummer's method. In a typical reaction, 5 g of EG, 60 mL of H_3PO_4, and 240 mL of H_2SO_4 were stirred together with a Teflon-coated magnetic stirrer in an ice bath. Next, 60 g of $KMnO_4$ was slowly added while the temperature was maintained at 0 °C. Once mixed, the solution was transferred to a 35 ± 5 °C water bath and stirred for 3 h, forming a thick paste. Next, distilled water (450 mL) was slowly dropped into the resulting paste to dilute the mixture, and then the solution was stirred for 1 h while the temperature was raised to 90 ± 5 °C. Finally, 800 mL of distilled water was added, followed by the slow addition of 60 mL H_2O_2 (30%), turning the color of the solution from dark brown to yellow. During this final step, H_2O_2 (30%) reduced the residual permanganate and manganese dioxide to colorless soluble manganese sulfate. The GO deposit was collected from the GO suspension by high speed centrifugation, at 15,000 rpm for 30 min. The obtained GO was then washed with 1000 mL of HCl (5%), and repeatedly washed with distilled water until the pH = 7. To obtain uniform GO, a low-speed centrifugation at 3000 rpm was first used to remove thick multilayer sheets until all the visible particles were removed (3–5 min). Then the supernatant was further centrifuged at 10,000 rpm for 30 min to remove small GOpieces and water-soluble byproduct. Next, the obtained GO was dried and stored in a vacuum oven at 90 °C until use. The exfoliated GO nanosheets were chemically reduced to graphene in the presence of hydrazine. Typical, 500 ml of above exfoliated GO was stirred for 30 min, and 50 ml of hydrazine monohydrate was added. The mixtures were heated at 150 ± 5 °C using an oil bath for 48 h; a black solid precipitated (called RGO) from the reaction mixtures. Products were collected by centrifugation at 12,000 rpm for 45 min and washed with DI water and methanol until the pH = 7.

The synthesized products were characterized by using a field-emission scanning electron microscope (FE-SEM, JSM-6700, JEOL Ltd., Tokyo, Japan) operated at an accelerating voltage of 12 kV. Transmission electron microscope (TEM) images were obtained on a JEOL JEM-2010 TEM (JEOL Ltd., Tokyo, Japan) with an accelerating voltage of 200 kV. Atomic force microscope (AFM) images were obtained on an AFM XE-100 (Park system) equipment. Optical microscope (OM) examination was carried on a Zeiss AX10 microscope. X-ray diffraction (XRD) characterization was obtained using a D/MAX Rint 2000 diffractometer model (Rigaku, Tokyo, Japan) with Cu Kα radiation (λ = 1.54178 Å, 40 kv, 200 mA). The Raman spectra were taken using a Jasco Laser Raman Spectrophotometer NRS-3000 Series, with excitation laser wavelength and power density of532 nm and 2.9 mW cm^{-2}, respectively. X-ray photoelectron spectroscopy (XPS, VG Multilab ESCA 2000 system, UK) analysis using a monochromatized Al Kα X-ray source ($h\nu$ = 1486.6 eV) was performed to analyze the elemental compositions and the assignments of the carbon peaks of the samples at the Korean Basic Science Institute. The Fourier transform infrared (FTIR) spectra (500–4000 cm^{-1}) were obtained using a Nicolet IR100 FTIR spectrometer. The Ultraviolet–visible (UV–vis) absorption spectra were performed on a Shimazu UV-3600 Ultraviolet–visible-near infrared (UV–vis-NIR) spectrophotometer at room temperature. The current–voltage (I-V) characteristics of the samples were measured by the four probe method within an applied voltage ranging from −1.0 to 1.0 V using a source meter (KeithleyModel 2400, OH, USA).

3. Results and discussion

Fig. 1 shows typical FE-SEM images of the as-made GO sheets. From Fig. 1a, the thin wrinkled accordion- or worm-like structure morphology of the GO sheets can be observed. This material consists of randomly aggregated, thin and wrinkled sheets, being loosely associated with each other. Most of the GO has been efficiently exfoliated to single or few-layer GO sheets in the present work. Fig. 1b shows a high-resolution FE-SEM image of the GO. It is clearly seen that the GO sheets predominantly consist of single or double layer graphene, with some of them being overlapped. The edges of the sheets are partially folded so that the total surface energy can be reduced. In comparison to the GO, the FE-SEM images of the FLG in Figs.2a and b reveal that the FLG consist of randomly individual graphene sheets that are separated from each other. The size of the sheets ranged from 3 to 10 μm. Fig. 2c shows the moderate-magnification FE-SEM image of single layer graphene sheets. Fig. 2d displays a high magnification FE-SEM image of a single layer graphene sheet. It clearly shows the wrinkles on the surface and folding at the edges of graphene sheet. Fig. 3 show the typical OM images of FLG sheets with the size in range of 5–7 μm, which are in quite agreement with the SEM results.

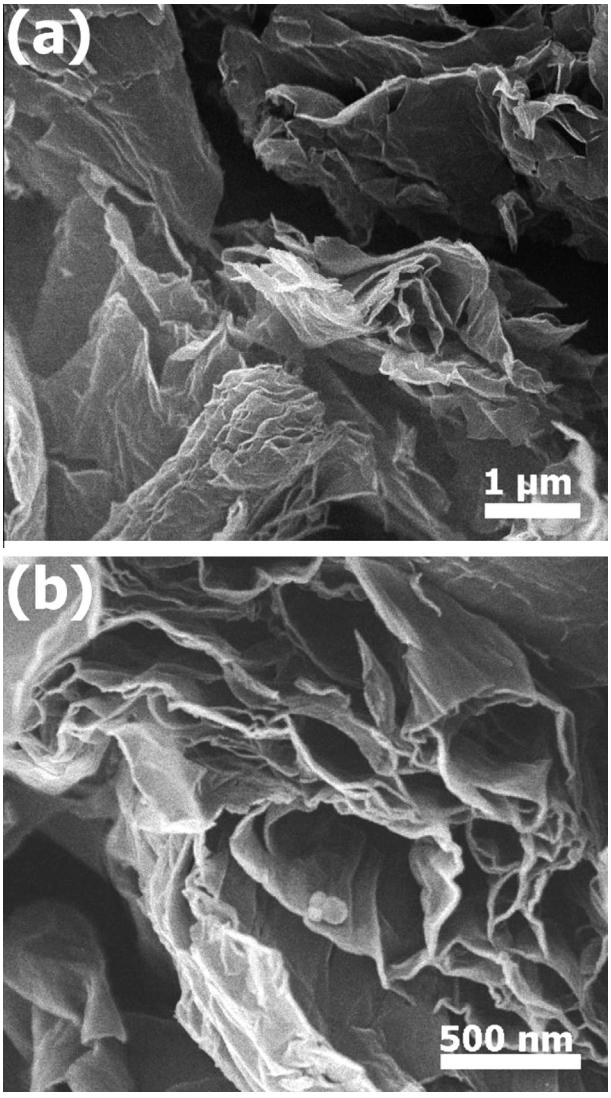

Fig. 1. (a) Low magnification and (b) high magnification FE-SEM images of as-fabricated GOs.

Fig. 4 shows typical TEM images of the as-synthesized GO (a and b) and FLG (c and d). As shown in Fig. 4a, the transparent GO sheets with wrinkled feature are easily observed. The as-prepared GO sheets are single-layer- or double-layer-thick with lateral dimensions from several micrometers to several ten micrometers. The electron diffraction pattern in Fig. 4a indicates that the formed GO corresponds to the ordered stage structure rather than the amorphous structure. The high-resolution TEM image of a single layer GO sheet is shown in Fig. 4b. It clearly shows that the GO sheet is folded at the edges with numerous wrinkles on its surface. Fig. 4c shows some bi-layergraphene sheets with many ripples and wrinkles on their surface, and most of them are folded at their edges [22]. The electron diffraction patterns in Fig. 4c of FLG are comprised of a single set of hexagonal patterns similar to those commonly observed in single-layer graphene and GO [23,24], indicating that the obtained FLG are well-crystallized. Fig. 4d reveals the TEM image of a single-layer graphene sheet with lateral dimensions of 2–5 μm, and how the edge tends to scroll.

The morphology and thickness of GO and FLG were also measured by AFM and the results are shown in Fig. 5. The AFM image of GO shows nanosheets with wrinkles on their surface. The thickness of the GO obtained from the height profile analysis of AFM image is about 1.2 nm, which suggests that the single or double-layer GO nanosheets are formed because the thickness of a one layer GO nanosheet is about 0.8–1.6 nm [25–27]. Such thickness is significantly larger than that of single-layer pristine graphene (~0.34 nm) and is commonly attributed to the presence of oxygen-containing functional groups attached on both sides of the graphene sheet and to the atomic scale roughness arising from structural defects (sp^3 bonding) generated on the originallyatomically flat graphene sheet [28]. Thus, individual GO sheets are expected to be thicker (~0.8–1.6 nm) than individual pristine graphene sheets (~0.34 nm).

In the case of FLG, a two dimensional AFM image is shown in Fig. 5b. It is found that the thickness of sheets obtained is about 1.8–2 nm, which is larger than the thickness of double-layer graphene (1.22 nm) [29]. Considering the oxygen-containing functional groups that are on both sides of the graphene, the products are double-layer graphene. The three dimensional AFM image reveals the FLG with uniform thickness and a homogenous smooth surface, as seen in Fig. 5c. It is clear that the FLG synthesized by our method are nanosized in the vertical direction and microsized in the horizontal direction.

Fig. 6a shows the XRD patterns of EG, GO, RGO and FLG. The EG shows the very strong (002) peak at $2\theta = 26.10°$, corresponding to interlayer distance (*d*-spacing) of about 3.40 Å (estimated from the Bragg equation). However, after the oxidation of EG to GO, the (002) peak shifted to a lower angle of around $2\theta = 11.15°$ and the *d*-spacing of GO increased to 7.90 Å. Such *d*-spacing is significantly larger than that of single-layer graphene (~3.35 Å), indicating that GO contains large numbers of oxygen-containing functional groups on both sides of the graphene sheets. Inaddition, some small bumps near 22° and 26° indicate that the GO has not been completely oxidized. For RGO sample, the peak disappeared in a region of low angle and another broad peak at 21.31° corresponding to *d*-spacing of 3.50 Å appeared. This indicated that a large number of functional groups on the surface of GO was removed during chemical reduction process. In contrast, in the diffraction pattern of FLG shows a strong and sharp (002) peak at around $2\theta = 26.23°$ corresponding to *d*-spacing of 3.39 Å, which is very close to that of conventional graphene (~3.35 Å). That implies that there are only a few oxygen functional groups in the interlayer of the FLG, demonstrating the effectiveness of the solvothermal method.

FTIR analysis of the as-made samples was carried out to provide compositional and structural information of the samples. Fig. 6b shows FTIR spectra of EG, GO, RGO and FLG. In the spectrum of

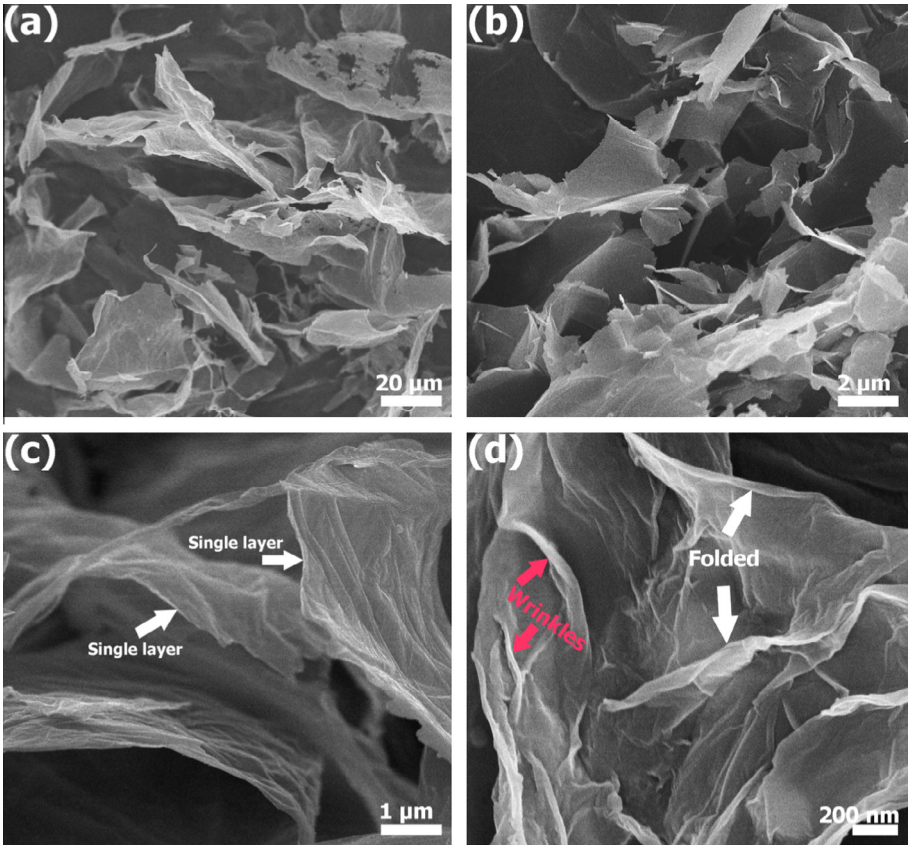

Fig. 2. (a) Low-magnification, (b and c) moderate-magnification and (d) high-magnification FE-SEM images of FLG.

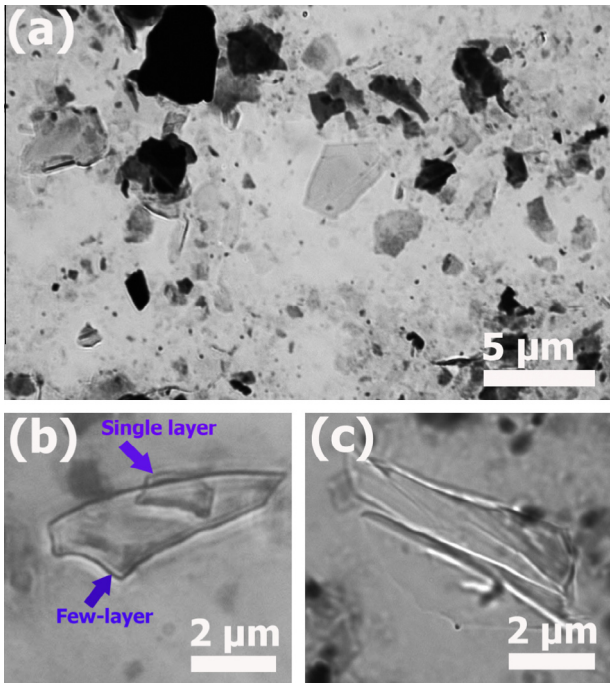

Fig. 3. OM images of FLG, (a) low-magnification and (b and c) high-magnification.

EG, the peak at 1699 cm^{-1} can be attributed to the stretching vibration of C=O [30]. The strong peak at 1531 cm^{-1} can be ascribed to the vibration of aromatic C=C [31]. The spectrum also shows two peaks at 1218 and 1061 cm^{-1}, being originated from the C—O stretching vibrations of epoxy and alkoxy, respectively [30,32]. Finally, the peak at 1342 cm^{-1} can be due to the variations of tertiary C—OH groups [30]. This result suggests that a certain number of oxygen functional groups have been introduced into the carbon frameworks of the EG material. It is certain that some degree of intercalation occurs in EG, and these intercalation sites provide a path for K^+ species. After oxidation of EG to GO, new peaks appear at 3350 and 1374 cm^{-1}, corresponding to the O—H stretching vibration of adsorbed water molecules, and O—H deformation vibration mode, respectively [30]. The peak at 1614 cm^{-1} is attributed to the O—H bending vibration of absorbed water molecules and contributions from the vibration of aromatic C=C [33]. The peak at 1153 cm^{-1} can be attributed to C—O stretching of the ester group [34]. The spectrum of GO also shows a stretching vibration of C=O at 1723 cm^{-1}, which is slightly shifted to higher wave-number, being compared with that of the EG. Note that the peak at around 1531 cm^{-1} (C=C bonds) disappears, indicating that the harsh oxidation led to the loss of the structural integrity of the graphite. In the FT-IR spectrum of the RGO, the peaks at 1614, 1374 and 1218 cm^{-1} disappeared. The intensity of peak at 1061, 1727 and broad peak at 3480 cm^{-1} was markedly reduced, indicating the removal of the hydroxyl and carboxylic acid groups. It did not completely disappear because of the mild reaction conditions. In addition, there are three new bands at 1551, 1408 and 1194 cm^{-1} appeared in the spectrum of RGO. The band at 1551 corresponds to aromatic C=C bonds. The two bands at 1408 and 1194 can be attributed to sp^3 C—N and C—N stretching modes, respectively. Nevertheless, in the case of FLG, the peaks appear to be very similar to that of EG, suggesting that their original pristine structure has been retained in the final products. In addition, the peak intensity of oxygen functional groups of FLG (even some of them disappear) is much lower than those of GO and EG,

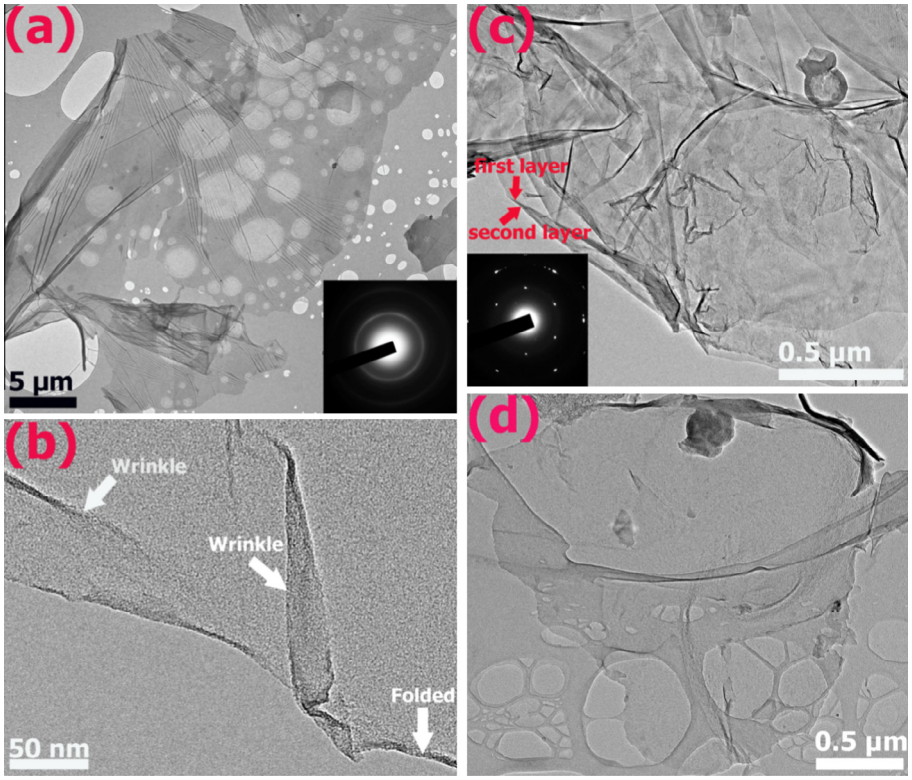

Fig. 4. (a) TEM images of GO. The inset in Fig. 4a is the corresponding selected area electron diffraction pattern (SAED). (b) HRTEM image of GO. (c) TEM image of FLG. The inset in Fig. 4c is the corresponding SAED. (d) TEM image of single-layer graphene.

suggesting the effectiveness of the solvothermal process in removing oxygen functional groups residing on the surface of the EG.

Fig. 7a shows the UV–vis spectra of GO and FLG dispersed in distilled water. The spectra of GO shows a high peak at 229 nm corresponding to the $\pi \rightarrow \pi^*$ transition of aromatic C=C bonds and a small shoulder at 299 nm, which can be attributed to the $n \rightarrow \pi^*$ transition of C=O bonds [35]. Only an intensity peak is observed at 269 nm for FLG, and the shoulder peak near 299 nm disappears. A large redshift of 40 nm in the absorption band of FLG compared with that of GO suggests that the π-conjugation within the FLG is less disrupted than that of GO [36,37]. A similar result has been observed in the previous study [38].

Raman spectroscopy is usually used to characterize carbon materials. Fig. 7b shows the Raman spectra of EG, FLG, RGO and GO. The EG has a prominent G band at 1583 cm^{-1}, which is assigned to the first-order scattering of the E_{2g} mode, being related to sp^2 carbon domains. Also, it has a broad D band at 1356 cm^{-1}, being caused by sp^3-hybridized carbon, structural defects, carbon amorphous or edge planes that can break the symmetry and selection rule [39]. In the Raman spectrum of GO, the G band is broadened and shifted to 1600 cm^{-1}, while the D band at 1354 cm^{-1} becomes prominent, indicating the destruction of the conjugated system in graphite due to harsh oxidation by strongacids during preparation. After GO was reduced to RGO, the D band became narrower and more prominent whilst the G band shifted from 1600 cm^{-1} to 1594 cm^{-1}, possibly due to increase of the number of sp^2 carbon in the graphene sheets. In contrast, in the Raman spectrum of FLG, the G band appears at 1583 cm^{-1}, which is consistent with the value in bulk EG, suggesting that the solvothermal process does not significantly disrupt the sp^2 carbon networks in the graphene sheets. It is worth noting that the D band of FLG also appears at a frequency of 1356 cm^{-1} and its intensity is higher than that of EG, but much lower than that of GO, indicating that the solvothermal method does not create significant structural defects. Our result is in good agreement with the previous study by Qian et al. [40]. The intensity ratio of D band to G band (I_D/I_G) is usually used to measure the graphitization degree of carbon materials. The I_D/I_G is estimated to be about 0.14, 0.23, 0.86 and 1.0 for EG, FLG, GO and RGO respectively. The I_D/I_G ratio of GO, RGO is much higher than that of EG and FLG, clearly indicating that GO and RGO has a higher distortion. The size of the sp^2 carbon domains (designated as La) can be calculated from the intensity ratio between D and G band in the Raman spectra using Knight's empirical formula [41].

$$La = 4.35(I_D/I_G)^{-1} \quad (1)$$

The calculated size of sp^2 domains is estimated to be ~31, 18, 5 and 4 nm for EG, FLG, GO and RGO, respectively. After harsh oxidation process, the size of sp^2 carbon domain decreased from ~31 nm for EG to ~5 nm for GO, indicating destruction of the sp^2 atomic structure graphite. Furthermore, size of sp^2 carbon domain of RGO continuously decreased to ~4 nm, suggesting that the chemical reduction can easily cause nucleation of sp^2 domains in the sp^3 matrix and the density of small sp^2 nucleus increased, decreasing the average size of sp^2 domains. However, for FLG sheets, the size of sp^2 domain is about 18 nm, larger than that of GO and RGO, suggesting that the effectiveness of the solvothermal method for remaining size of sp^2 carbon domain in graphene sheets. It is believed that the size of the sp^2 domains plays a determining role in the electronic properties of the carbon material [42].

XPS is a powerful tool for identifying elemental composition in bulk materials. Furthermore, by analysis of binding energy (BE) values, we can detect the presence of oxygenated groups. Fig. 8a shows the XPS survey spectra of EG, GO, RGO and FLG. With only carbon, oxygen species being detected, the atomic percentage (at.%) of each element was calculated from the survey spectra and is summarized in Table 1. The oxygen content was found to decrease in the order of GO > RGO > EG > FLG, clearly indicating the

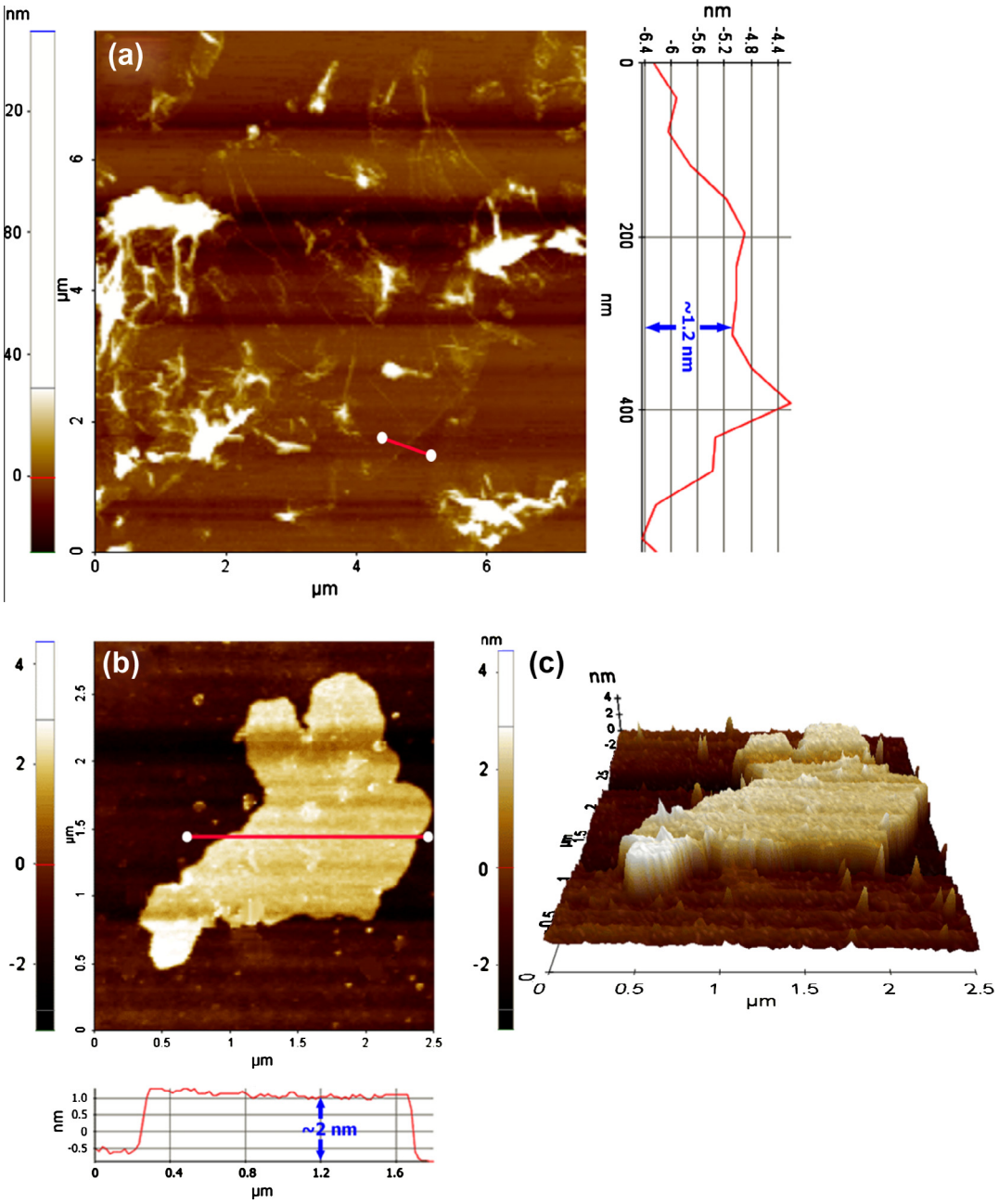

Fig. 5. (a) Two-dimensional AFM image of GO and the corresponding height profile (on the top right-side). (b) two- and (c) three-dimensional AFM images of FLG and the corresponding height profile (bottom).

effectiveness of the solvothermal method in lowering the oxygen and defect levels in graphene sheets [21]. In contrast, the GO produced by the Hummers' method can introduce many oxygen functional groups, such as COOH, —C═O, C—O—C, and —OH, onto the surfaces of graphene sheets; consequently, the obtained GO is an electrically insulating material. In the survey scan XPS spectra, the peaks at around 285.5 and 534.0 eV correspond to C1s and O1s core-level, respectively. Small peaks at around (100–160 eV) and (399–403 eV) are due to silicon substrate and N1s core-level, respectively. The N1s peak in the XPS spectrum of RGO can be ascribed to the formation of C—N species during hydrazine reduction.

It is known that the electronic structure of the graphene is strongly influenced by basal-plane or edge functionalization with oxygenated groups. In order to detect the presence of oxygenated groups, high-resolution C1s XPS spectra were measured and the results are shown in Fig. 8b–e. Note that the relative composition of individual groups was estimated by the percentage of the certain group (the area of peak divided by the total area of all peaks). For the EG, the C1s peak can be fitted to five components located at 284.8, 285.6, 286.4, 287.2 and 288.5 eV. The main peak at 284.7 eV corresponds to BE of sp^2 graphitic bonds (C═C), indicating that most of the carbon atoms in the EG are arranged in a conjugated honeycomb lattice (77.0% area of C═C bonds). The other four peaks located at 285.6, 286.4, 287.2 and288.5 eV are attributed to C—OH (hydroxyls), C-O-C (epoxy/ether), C═O (carbonyls), and COOH (acids) groups, respectively. The C1s XPS spectrum of GO clearly indicates a considerable degree of oxidation, with the content of oxygen element being increased to 25.2 at.% and the composition of C═C bonds decreasing to 62.4%, which results from the harsh oxidation and destruction of the sp^2 atomic structure

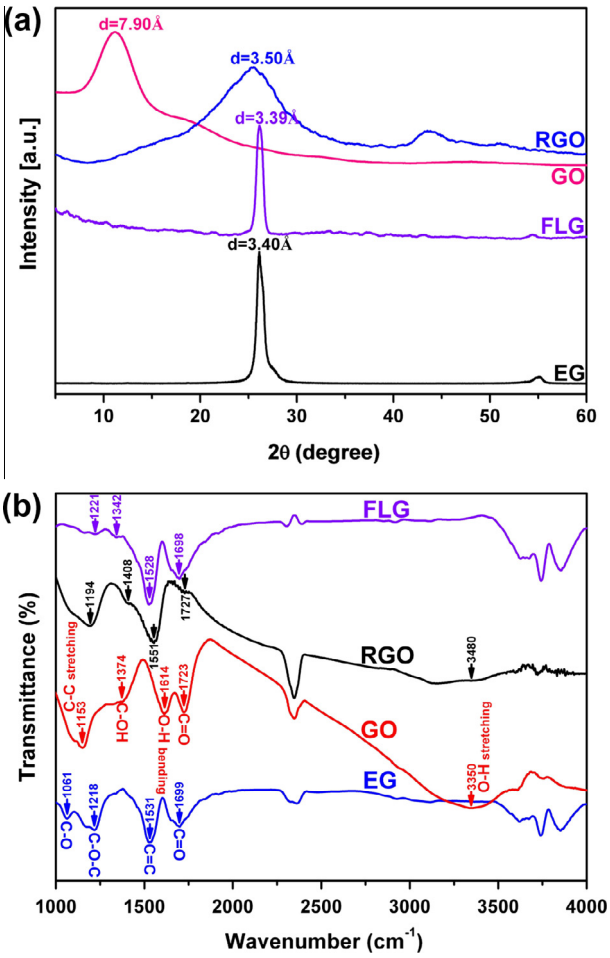

Fig. 6. (a) XRD patterns of EG, FLG, reduced graphene oxide (RGO) and GOs. (b) FTIR spectra of EG, FLG RGO and GOs.

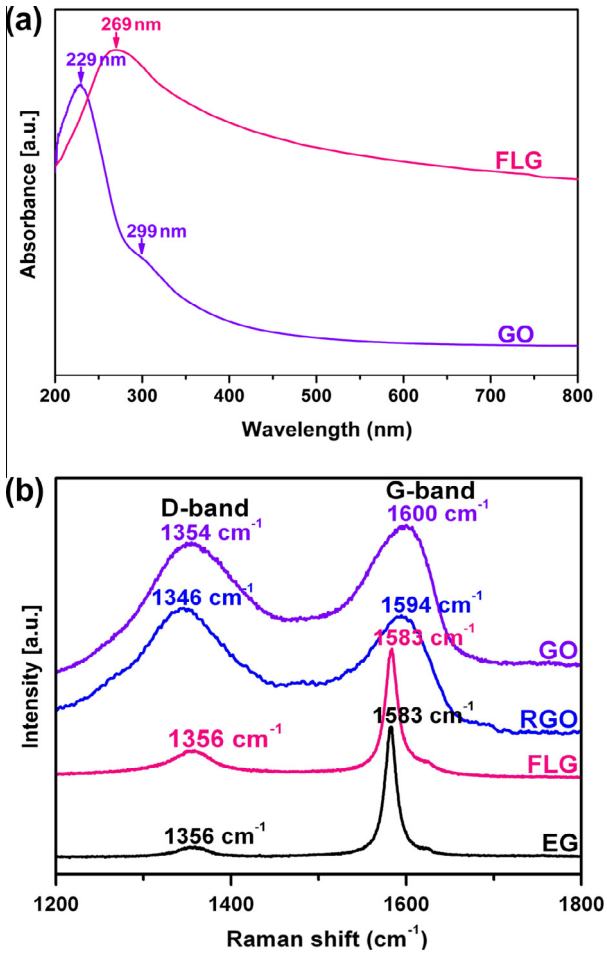

Fig. 7. (a) UV–vis spectra of FLG and GOs. (b) Raman spectra of EG, FLG, RGO and GOs.

graphite [43]. There are six different kinds of carbon atoms, located at 284.5, 285.6, 286.3, 287.5, 288.6, and 290.1 eV, correspondingly existing in different functional groups: C=C, C—OH, C—O—C, C=O, COOH and O=CO—O (carbonates) groups, respectively. This indicates that the rich oxygen groups are contained within the GO. For C1s XPS spectrum of RGO is found that oxygen functional groups (such as C—OH, C—O—C, C=O and COOH groups) of GO were considerably reduced after chemical reduction, while the composition of C=C bonds increased from 62.4% for GO, to 74.1% for RGO. At the same time, some new peaks ascribed to a C—N species, resulting from bond formation during hydrazine reduction, appeared at 286.2 and 288.0 eV in the RGO spectrum. In contrast to GO and RGO, FLG contains a very small amount of oxygen functional groups and some of them have even disappeared, while the composition of C=C bonds was increased up to 88.2%, which is higher than that of GO and EG and RGO. This indicates the effective restoration of the sp^2 carbon networks by the solvothermal method.

To examine the electrical conductivity of the as-made GO, RGO and FLG, we measured *I–V* characteristics by using four point probe with the Keithley 2400 Source-meter. In order to measure electrical conductivity, GO, RGO and FLG thin films of about 300 nm thickness were deposited on glass substrates ($2 \times 2\ cm^2$) from the GO, RGO and FLG suspension using air-brush spraying technique [44]. Next, these films were dried in a vacuum oven at 90 °C for 24 h. Fig. 9 shows the *I–V* characteristic of GO, RGO and FLG. It is found that all samples exhibit linear *I–V* relation with the voltage in the range of −1.0 to +1.0 V. From the linear *I–V* curves, the conductivities of 1.2×10^{-4}, 86 and 165 S/m were calculated for GO, RGO and FLG, respectively. The result shows that the GO behaved like an insulating material [45], which can be attributed to the high oxygen content in the form of functional groups contained by the GO. It is well-known that the GO structure is predominantly amorphous due to distortions from the high fraction of sp^3–O. Moreover, due to the random distribution, the sp^2-hybridized benzene rings are separated by sp^3-hybridized rings, thus leading to the insulating GO [46].The *I–V* slope of GO is close to zero. However, the *I–V* slope of RGO significantly increased after chemical reduction, indicating that the electrical conductivity of RGO was enhanced. The enhanced electrical conductivity of RGO can be due to chemical removal of oxygen functional groups during chemical reduction. Interestingly, it was found that the electrical conductivity of FLG is dramatically improved, approximately 6 orders higher than that of GO and two times higher than that of RGO, which is considerably higher than those prepared by other methods (50–100 S/m) [47,48], demonstrating the effectiveness of our method. The dramatic enhancement of conductivity of FLG can be due to the lower oxygen content and structural defect levels in graphene sheets, as shown by the Raman and XPS analyses.

It is believed that the concentration and size of sp^2 carbon domains play very important roles in controlling the electrical properties of the graphene sheets. In fact, it is shown that the high conductivity of the graphene films resulted from the improved sp^2 carbon networks in the graphene sheets and the reduced interlayer distance between the graphene sheets in the films [49]. Zhan

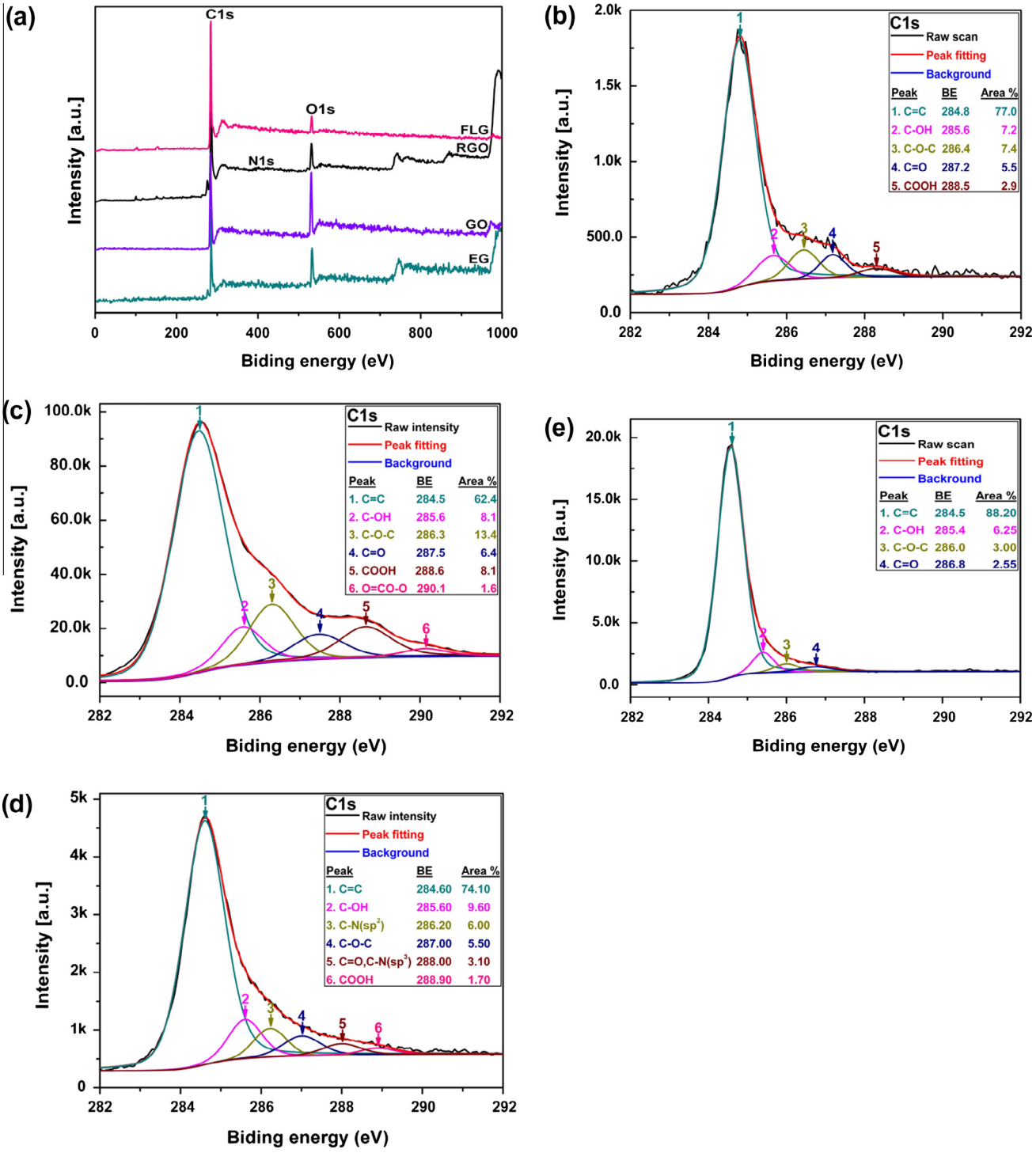

Fig. 8. (a) Raw scan XPS spectra of EG, GO, RGO and FLG; and high resolution C1s XPS spectra of (b) EG, (c) GO, (d) RGO and (e) FLG. The insets in Fig. 7b–e shows the possible chemical bonds between carbon and oxygen, and the corresponding composition of individual groups (area%) deduced from the deconvolution of C1s line.

Table 1
Atomic concentration of C and O of EG, GO and FLG, and corresponding size of sp^2 domains.

Sample	Atomic concentration			Size of sp^2 domains (nm)
	C (%)	O (%)	N (%)	
EG	78.5	21.5	–	~31
GO	68.8	31.2	–	~5
RGO	76.8	22.0	1.2	~4
FLG	93.5	6.5	–	~18

et al. [50] reported that the dramatic enhancement of conductivity of thermally reduced graphite oxide is due to the restoration of sp^2 hybridized carbon component and the removal of oxygenated functional groups. Moreover, Mattevi et al. [51] showed that the conductivity of thermally reduced GO increased with increasing the sp^2 carbon fraction. These studies suggest that the conductivity of graphene material depends on the quality of graphene sheet, i.e., it depends mainly on the concentration and size of sp^2 carbon domain in the graphene sheets. In our study, according to the XPS results (Fig. 8), the C=C component of GO, RGO and FLG sheet

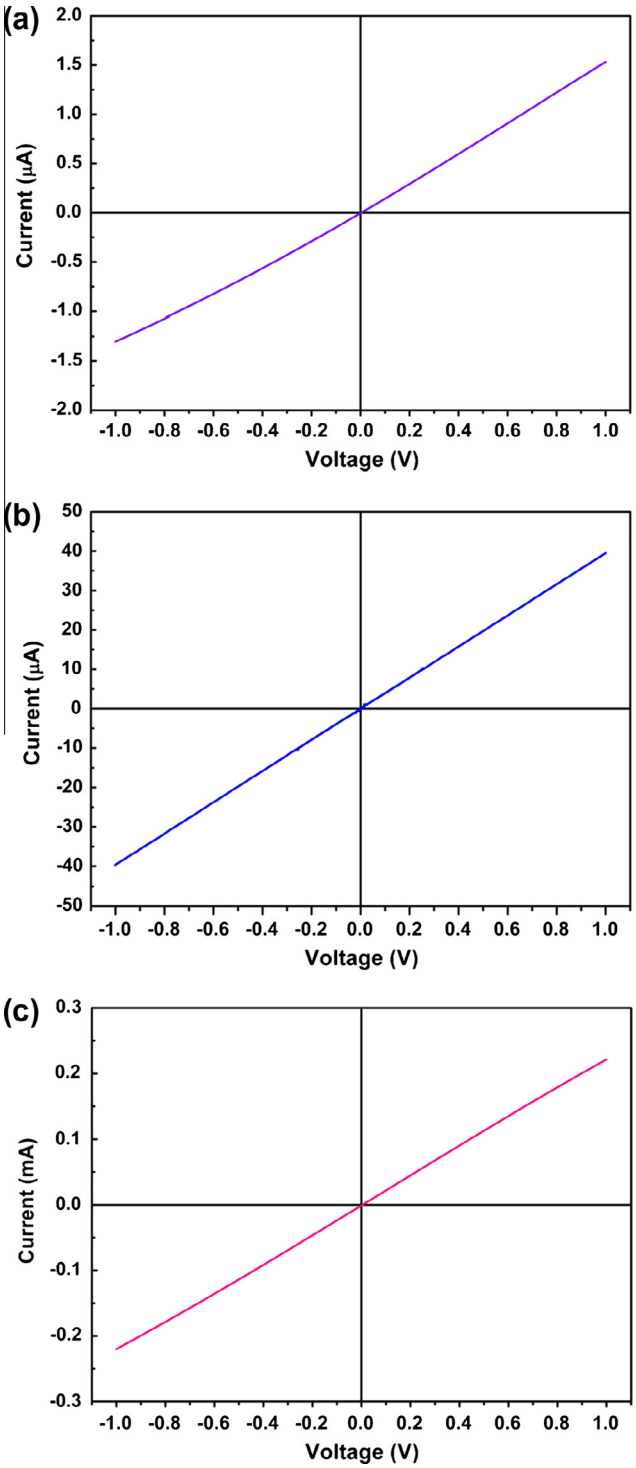

Fig. 9. Current–voltage (I–V) curves of (a) GO, (b) RGO and (c) FLG.

is estimated to be about: 62.4%, 74.1% and 88.2%, respectively. At the same time, the size of sp^2 carbon of GO, RGO and FLG sheet is calculated to be 5, 4 and 18 nm (see Table 1, according to Raman data in Fig. 7b), respectively. Furthermore, high resolution TEM is also performed to analyze size of sp^2 carbon domain of GO and FLG sheets and the results are shown in Fig. 10. From Fig. 10a–c, it is seen that GO consist of ~2–5 nm sp^2 carbon domains isolated within sp^3 carbon matrix. This is in accordance with the previous observation, revealing the size of the sp^2 domain of GO to be about 2.5–8 nm [51–53]. As shown in Fig. 10d, a higher concentration and larger size of sp^2 carbon domains (~10–16 nm) is observed

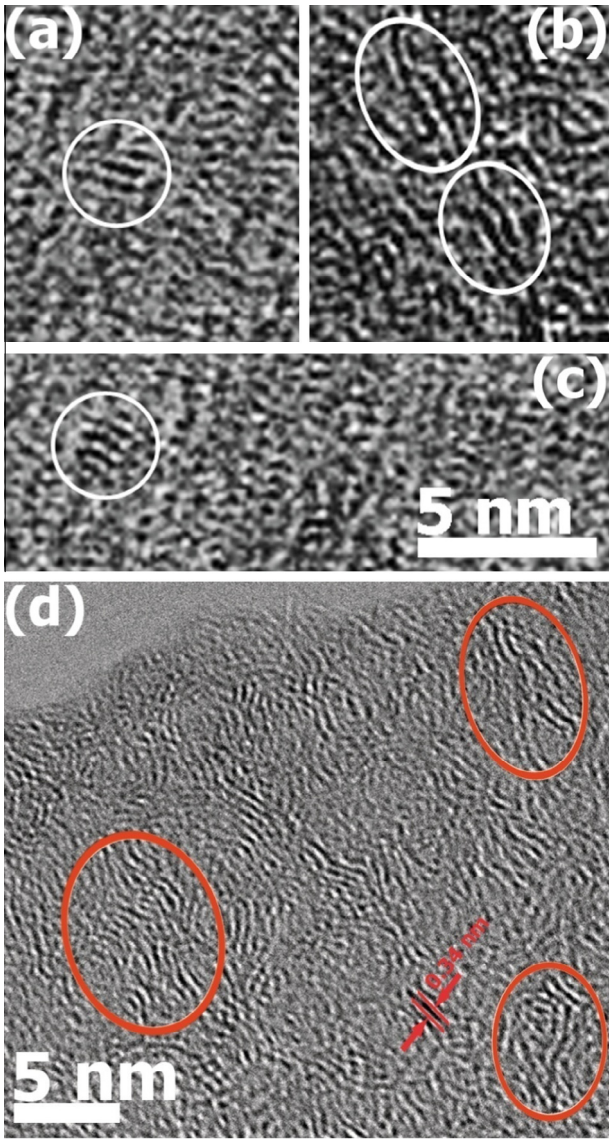

Fig. 10. HR-TEM images showing the microstructure of (a–c) GO and (d) FLG. Sp^2 carbon domains are indicated by ellipses. The size of sp^2 carbon domains of GO and FLG is about 2–5 and 10–16 nm, respectively.

in the FLG, in good agreement with the XPS and Raman results. It is believed that the higher concentration and larger size of the sp^2 carbon domains in the FLG leads to an increase in the number of conductive pathways, resulting in a dramatic increase in the electrical conductivity [8,51]. In addition, it was also shown that the electrical conductivity of graphene is directly related to the oxygen content [47]. In the present case, the C/O ratio of FLG is calculated to be 14.4, which is much higher than that of GO (2.2). By considering all these factors, we conclude that the higher electrical conductivity of FLG is due to larger size of sp^2 carbon domains and higher C/O ratio.

4. Conclusions

In conclusion, we reported a simple method of preparing few-layer graphene sheets having low oxygen and structural defects levels, through a solvothermal process followed by microwave-assisted expansion, using EG as starting material. This method has the following advantages: (1) it can be applied to produce few-layer (2–3 layers) graphene sheets with a lateral size up to several micrometers; (2) the obtained FLG has higher C/O ratio and lower

structural defect level (compared to those of chemical reduction or thermal reduction of GO); (3) the method provides an alternative route for producing large-scale high quality graphene sheets; (4) this method avoids the use of toxic and harmful reducing agents, such as hydrazine, dimethyl hydrazine and hydroquinone. The as-fabricated graphene sheets exhibited a high electrical conductivity of ~165 S/m, which can open up a wide range of applications in technology fields, such as ultra-sensitive gas sensor,transparent electrodes, solar cell, field effect transistors and graphene-based composites.

Acknowledgements

This work was supported by the National Research Foundation of Korea (NRF) grant funded by the Korea government(MEST) (No. 2012029262 and the National Foundation for Science and Technology Development (NAFOSTED), Vietnam.

References

[1] A.K. Geim, K.S. Novoselov, The rise of grapheme, Nat. Mater. 6 (2007) 183–191.
[2] C. Lee, X. Wei, J.W. Kysar, J. Hone, Measurement of the elastic properties and intrinsic strength of monolayer graphene, Science 321 (2008) 385–388.
[3] A.A. Balandin, S. Ghosh, W.H. Bao, I. Calizo, D. Teweldebrhan, F. Miao, C. Lau, Superior thermal conductivity of single-layer grapheme, Nano Lett. 8 (2008) 902–907.
[4] K.I. Bolotin, K.J. Sikes, Z. Jiang, M. Klima, G. Fudenberg, J. Hone, P. Kim, H. Stormer, Ultrahigh electron mobility in suspended grapheme, Solid State Commun. 146 (2008) 351–355.
[5] M.D. Stoller, S. Park, Y. Zhu, J. An, R.S. Ruoff, Graphene-based ultracapacitors, Nano Lett. 8 (2008) 3498–3502.
[6] Y. Zhang, Y.W. Tan, H.L. Stormer, P. Kim, Experimental observation of the quantum Hall effect and Berry's phase in graphene, Nature 438 (2005) 201–204.
[7] W.S. Kim, S.Y. Moon, S.Y. Bang, B.G. Choi, H. Ham, T. Sekino, K. Shim, Fabrication of graphene layers from multiwalled carbon nanotubes using high dc pulse, Appl. Phys. Lett. 95 (2009) 083103.
[8] V.C. Tung, M.J. Allen, Y. Yang, R.B. Kaner, High-throughput solution processing of large-scale grapheme, Nature 4 (2009) 25–29.
[9] C. Berger, Z. Song, X. Li, X. Wu, N. Brown, C. Naud, D. Mayou, T. Li, J. Hass, A. Marchenkov, E. Conrad, P. First, W. de Heer, Electronic confinement and coherence in patterned epitaxial grapheme, Science 312 (2006) 1191–1196.
[10] M. Eizenberg, J.M. Blakely, Carbon monolayer phase condensation on. Ni(111), Surf. Sci. 82 (1970) 228–236.
[11] X. Lu, M. Yu, H. Huang, R.S. Ruoff, Tailoring graphite with the goal of achieving single sheets, Nanotechnology 10 (1999) 269.
[12] S. Park, J. An, R.D. Piner, I. Jung, D. Yang, A. Velamakanni, S. Nguyen, R. Ruoff, Aqueous suspension and characterization of chemically modified graphene sheets, Chem. Mater. 20 (2008) 6592–6594.
[13] W.S. Hummers, R.E. Offeman, Preparation of graphitic oxide, J. Am. Chem. Soc. 80 (1958) 1339.
[14] A. Lerf, H. He, M. Forster, J. Kliowski, Structure of graphite oxide revisited, J. Phys. Chem. B 102 (1998) 4477–4482.
[15] H.Y. He, T. Riedl, A. Lerf, J. Klinowski, Solid-state NMR studies of the structure of graphite oxide, J. Phys. Chem. 100 (1996) 19954–19958.
[16] Q. Liang, X. Yao, W. Wang, Y. Liu, C.P. Wong, A three-dimensional vertically aligned functionalized multilayer graphene architecture: an approach for grpahene-based thermal interfacial materials, ACS Nano 5 (2011) 2392–2401.
[17] M. Choucair, P. Thordarson, J.A. Stride, Gram-scale production of graphene based on solvothermal synthesis and sonication, Nat. Nanotechnol. 4 (2008) 30–33.
[18] C. Nethravathi, M. Rajamathi, Chemically modified graphene sheets produced by the solvothermal reduction of colloidal dispersions of graphite oxide, Carbon 46 (2008) 1994–1998.
[19] S. Dubin, S. Gilje, K. Wang, V.C. Tung, K. Cha, A.S. Hall, J. Farrar, R. Varshneya, Y. Yang, R. Kaner, A one-step, solvothermal reduction method for producing reduced graphene oxide dispersions in organic solvents, ASC Nano 4 (2010) 3845–3852.
[20] Q. Liang, S.A. Hsie, C.P. Wong, Low-temperature solid-state microwave reduction of graphene oxide for transparent electrically conductive coatings on flexible polydimethylsiloxane (PDMS), Chem. Phys. Chem. 13 (2012) 3700–3706.
[21] H. Wang, J.T. Robinson, X. Li, H. Dai, Solvothermal reduction of chemically exfoliated graphene sheets, J. Am. Chem. Soc. 131 (2009) 9910–9911.
[22] A.C. Ferrari, J.C. Meyer, V. Scardaci, C. Casiraghi, M. Lazzeri, F. Mauri, Raman spectrum of graphene and graphene layers, Phys. Rev. Lett. 97 (2006) 187401.
[23] J.C. Meyer, A.K. Geim, M.I. Katsnelson, K.S. Novoselov, T.J. Booth, S. Roth, The structure of suspended graphene sheets, Nature 446 (2007) 60–63.
[24] N.R. Wilson, P.A. Pandey, R. Beanland, R.J. Young, I.A. Kinloch, L. Gong, Z. Liu, K. Suenaga, J. Rourke, S. York, J. Sloan, Graphene oxide: structural analysis and application as a highly transparent support for electron microscopy, ACS Nano 3 (2009) 2547–2556.
[25] L. Zhang, J.J. Liang, Y. Huang, Y.F. Ma, Y. Wang, Y.S. Chen, Size-controlled synthesis of graphene oxide sheets on a large scale using chemical exfoliation, Carbon 47 (2009) 3365–3380.
[26] L. Zhang, X. Li, Y. Huang, Y.F. Ma, X.J. Wan, Y.S. Chen, Controlled synthesis of few-layered graphene sheets on a large scale using chemical exfoliation, Carbon 48 (2010) 2367–2371.
[27] K.A. Mkhoyan, A.W. Contryman, J. Silcox, D.A. Stewart, G. Eda, C. Mattevi, S. Miller, M. Chhowalla, Atomic and electronic structure of graphene-oxide, Nano Lett. 9 (2009) 1058–1063.
[28] S. Stankovich, D.A. Dikin, R.D. Piner, Kevin A. Kohlhaas, Y. Kleinhammes, Y. Jia, Y. Wu, S.B.T. Nguyen, R.S. Ruoff, Synthesis of graphene-based nanosheets via chemical reduction of exfoliated graphite oxide, Carbon 45 (2007) 1558–1565.
[29] Z.S. Wu, W. Ren, L. Gao, B. Liu, C. Jiang, H.M. Cheng, Synthesis of high-quality graphene with a pre-determined number of layers, Carbon 47 (2009) 493–499.
[30] C. Hontorialucas, A.J. Lopezpeinado, J.D.D. Lopezgonzalez, M.L. Rojascervantes, R.M. Martinaranda, Study of oxygen-containing groups in a series of graphite oxides: physical and chemical characterization, Carbon 33 (1995) 1585–1592.
[31] A.K. Mishra, S. Ramaprabhu, Removal of metals from aqueous solution and sea water by functionalized graphite nanoplatelets based electrodes, J. Hazard. Mater. 185 (2011) 322–328.
[32] V. Chandra, K.S. Kim, Highly selective adsorption of Hg^{2+} by polypyrrole-reduced graphene oxide composite, Chem. Commun. 47 (2011) 3942–3944.
[33] Y.X. Xu, H. Bai, G.W. Lu, C. Li, G.Q. Shi, Flexible graphene films via the filtration of water-soluble noncovalent functionalized graphene sheets, J. Am. Chem. Soc. 130 (2008) 5856–5857.
[34] Q. Wei, X. Wang, F. Zhou, A versatile macro-initiator with dual functional anchoring groups for surface-initiated atom transfer radical polymerization on various substrates, Polym. Chem. http://dx.doi.org/10.1039/c2py20148h.
[35] J.I. Paredes, S. Villar-Rodil, A. Martinez-Alonso, J.M.D. Tascon, Graphene oxide dispersions in organic solvents, Langmuir 24 (2008) 10560–10564.
[36] D. Li, M.B. Muller, S. Gilje, R.B. Kaner, G.G. Wallace, Processable aqueous dispersions of graphene nanosheets, Nat. Nanotechnol. 3 (2008) 101–105.
[37] Y. Hernandez, High-yield production of graphene by liquid-phase exfoliation of graphite, Nat. Nanotechnol. 3 (2008) 563–568.
[38] P.L. Chiu, D.D.T. Mastrogiovanni, D. Wei, C. Louis, M. Jeong, G. Yu, P. Saad, C. Flach, R. Mendelsohn, E. Garfunkel, H. He, Microwave- and nitronium ion-enabled rapid and direct production of highly conductive low-oxygen grapheme, J. Am. Chem. Soc. 134 (2012) 5850–5856.
[39] A.C. Ferrari, J.C. Meyer, V. Scardaci, C. Casiraghi, M. Lazzeri, F. Mauri, S. Piscanec, D. Jiang, K. Novoselov, S. Roth, A. Geim, Raman spectrum of graphene and graphene layers, Phys. Rev. Lett. 97 (2006) 187401.
[40] W. Qian, R. Hao, Y. Hou, Y. Tian, C. Shen, H. Gao, X. Liang, Solvothermal-assisted exfoliation process to produce graphene with high yield and high quality, Nano Res. 2 (2009) 706–712.
[41] F.C. Tai, C. Wei, S.H. Chang, W.S. Chen, Raman and X-ray diffraction analysis on unburned carbon powder refined from fly ash, J. Raman Spectrosc. 41 (2010) 933–937.
[42] J.D. Carey, S.R.P. Silva, Disorder, domaining, and localization effects in amorphous carbon, Phys. Rev. B 70 (2004) 235417.
[43] B.J. Jiang, C.G. Tian, L. Wang, Y.X. Xu, R.H. Wang, Y.J. Qiao, Y. Ma, H. Fu, Facile fabrication of high quality graphene from expandable graphite: simultaneous exfoliation and reduction, Chem. Commun. 46 (2010) 4920–4922.
[44] T.V. Khai, H.G. Na, D.S. Kwak, Y.J. Kwon, H. Ham, K.B. Shim, H.W. Kim, Influence of N-doping on the structural and photoluminescence properties of graphene oxide films, Carbon 50 (2012) 3799–3806.
[45] C. Gómez-Navarro, R.T. Weitz, A.M. Bittner, M. Scolari, A. Mews, M. Burghard, K. Kern, Electronic transport properties of individual chemically reduced graphene oxide sheets, Nano Lett. 7 (2007) 3499–3503.
[46] P.G. Ren, D.X. Yan, X. Ji, T. Chen, Z.M. Li, Temperature dependence of graphene oxide reduced by hydrazine hydrate, Nanotechnology 22 (2011) 055705.
[47] H.J. Shin, K.K. Kim, A. Benayad, S.M. Yoon, H.K. Park, I.S. Jung, M. Jin, H. Jeong, J. Kim, J. Choi, Y. Lee, Efficient reduction of graphite oxide by sodium borohydride and its effect on electrical conductance, Adv. Funct. Mater. 19 (2009) 1987–1992.
[48] D. Zhan, Z. Ni, W. Chen, L. Sun, Z. Luo, L. Lai, T. Yu, A.T.S. Wee, Z. Shen, Electronic structure of graphite oxide and thermally reduced graphite oxide, Carbon 49 (2011) 1362–1366.
[49] J. Geng, L. Liu, S.B. Yang, S.C. Youn, D.W. Kim, J.S. Lee, J.K. Choi, H.T. Jung, A simple approach for preparing transparent conductive graphene films using the controlled chemical reduction of exfoliated graphene oxide in an aqueous suspension, J. Phys. Chem. C 114 (2010) 14433–14440.
[50] D. Zhan, Z.H. Ni, W. Chen, L. Sun, Z.Q. Luo, L.F. Lai, T. Yu, A.T.S. Wee, Z.X. Shen, Electronic structure of graphite oxide and thermally reduced graphite oxide, Carbon 49 (2011) 1362–1366.
[51] C. Mattevi, C. Eda, S. Agnoli, S. Miller, K.A. Mkhoyan, O. Celik, et al., Evolution of electrical, chemical, and structural properties of transparent and conducting chemically derived graphene thin films, Adv. Funct. Mater. 19 (2009) 2577–2583.
[52] K. Erickson, R. Erni, Z. Lee, N. Alem, W. Gannett, A. Zettl, Determination of the local chemical structure of graphene oxide and reduced graphene oxide, Adv. Mater. 22 (2010) 4467–4472.
[53] G. Eda, M. Chhowalla, Chemically derived graphene oxide: towards large-area thin-film electronics and optoelectronics, Adv. Mater. 22 (2010) 2392–2415.